Comparisons of IASI-A and AATSR measurements of top-of-atmosphere radiance over an extended period

Atmos. Meas. Tech., 9, 3325–3336, 2016
www.atmos-meas-tech.net/9/3325/2016/
doi:10.5194/amt-9-3325-2016

Atmospheric Measurement Techniques
Open Access
EGU

Comparisons of IASI-A and AATSR measurements of top-of-atmosphere radiance over an extended period

Manik Bali[1], **Jonathan P. Mittaz**[2], **Eileen Maturi**[3], **and Mitchell D. Goldberg**[3]

[1]ESSIC/CICS, University of Maryland, College Park, MD, USA
[2]Department of Meteorology, University of Reading, Reading, UK
[3]National Oceanic and Atmospheric Administration, College Park, MD, USA

Correspondence to: Manik Bali (manik.bali@noaa.gov)

Received: 21 July 2015 – Published in Atmos. Meas. Tech. Discuss.: 18 September 2015
Revised: 15 May 2016 – Accepted: 27 June 2016 – Published: 27 July 2016

Abstract. This study examines the trustworthiness of the Advanced Along-Track Scanning Radiometer (AATSR) and the Infrared Atmospheric Sounding Interferometer (IASI-A), as on-orbit reference instruments that are useful in re-calibrating the Advanced Very High Resolution Radiometer (AVHRR) series (Mittaz and Harris, 2011). To do this, a 39-month period (1 January 2008 to 31 March 2011) of AATSR and IASI-A inter-comparisons of top-of-atmosphere (TOA) radiance measurements is examined. Our inter-comparison reveals features of the AATSR and IASI-A bias with respect to scan angle, scene temperature, time and orbital maneuvers, and gives insight into their trustworthiness as an in-orbit reference instruments.

The first feature that our study reveals is that the AATSR (nadir view) and IASI-A are both stable (have no perceptible trends in the period of study). The second feature is that IASI-A is perhaps more accurate (~ 0.05 K) than its stated accuracy (0.5 K). In fact the AATSR and IASI-A bias is close to the AATSR pre-launch bias (plus a small offset of $+0.07$ K) implying that IASI-A can get close to pre-launch levels of accuracy. Third, a very small scan angular dependence of AATSR and IASI-A bias indicates that the IASI-A response vs. scan angle algorithm is robust, while the instrument is in orbit.

Inter-comparisons of AATSR with IASI-A further reveal the impact of orbital maneuvers of the ENVISAT, the platform carrying AATSR, done in October 2011 and not anticipated previously. Our study reveals that this maneuver introduced a temperature-dependent bias in the AATSR measurements for low temperatures (<240 K) in the period following this maneuver (Cocevar et al., 2011). Our study also shows that the known AATSR 12 µm channel offset is in fact temperature dependent, grows up to 0.4 K, varies seasonally and is correlated with instrument temperature and cannot be corrected by shifting the spectral response function (SRF) of AATSR.

We also present a set of recommendations to help identify the parameters under which these instruments can provide the most trustworthy observations for the AVHRR re-calibration.

1 Introduction

The launch of ENVISAT in 2002 and the launch of MetOp-A in 2006 put two highly accurate instruments in space to measure the top-of-atmosphere (TOA) radiances. These instruments are the Advanced Along-Track Scanning Radiometer (AATSR) and Infrared Atmospheric Sounding Instrument (IASI-A). The AATSR is able to measure brightness temperature (BT) to an accuracy of 30 mK (Illingworth et al., 2009). The IASI-A is a hyper spectral instrument that has a stated accuracy of 0.5 K (Illingworth et al., 2009).

Under the aegis of the Global Space-based Inter-Calibration System (GSICS) over 15 satellite agencies use IASI-A as a reference to monitor their in-orbit instruments by inter-comparing them with IASI-A in real time. Such inter-comparisons have helped detect anomalies and trends in monitored instruments and correct them (Hewison et al., 2013).

More recently the IASI-A has emerged as a crucial reference in re-calibration of legacy instruments such as the Ad-

vanced Very High Resolution Radiometer (AVHRR) series of instruments. Mittaz and Harris (2011) developed a new calibration scheme for the AVHRR series of instruments. This scheme uses IASI-A as a reference source and the inter-comparison of IASI-A with AVHRR to detect time, temperature and viewing-angle-dependent biases in AVHRR TOA radiance measurements. This scheme physically models the AVHRR biases and corrects them. This calibration scheme brings the AVHRR measurements close to the "climate readiness" i.e accuracy better than 0.1 K and its stability better than 0.05 K dec^{-1} (Ohring et al., 2005).

However the legacy of the AVHRR series goes back to 1978 and one needs a cascade of reference instruments prior to the launch of the IASI-A to re-calibrate AVHRRs launched prior to 2006. AIRS (Atmospheric Infrared Sounder), another commonly used hyper spectral sounding instrument dates back to 2002 only. Prior to that, the only credible TOA reference is the Along-Track Scanning Radiometer series, namely the ATSRs (ATSR-1 launched in 1991, ATSR-2 in 1995 and the AATSR in 2002). Hence in principle if one were to use a combination of the ATSR's AIRS and IASI-A (launched in 2006) one can get a reference radiance starting from the early 90s right until now. However one needs to evaluate how well these instruments can reveal the time, scene temperature, viewing-angle-dependent biases of the AVHRRs to have an opinion of their trustworthiness for use as a reference for re-calibration of AVHRR series. As a first step in this study we focus on the period from 2002 onwards and evaluate the trustworthiness of the AATSR and IASI-A in their role as a reference for re-calibration of AVHRR .

A previous study by Illingworth et al. (2009) used the AATSR as a benchmark and attempted to measure the bias in IASI-A vs. AATSR. Using a small number of collocations (41 for clear sky and 66 for homogenous scenes) taken from a single orbit on 1 September 2007 over oceans, this study concluded that the mean measurements for the 11 and 12 µm channels of IASI-A and AATSR measurements agree to within −0.05 and 0.23 K, respectively. The Illingworth study was sufficient to provide a basic estimate of differences between IASI-A and the AATSR. However in order to form an opinion about their use for re-calibration studies, key questions about the possible variations of bias with scan angle, scene temperature, time and spectrum still needed to be addressed. In addition, for the AATSR there is a known brightness temperature (BT) offset on the order −0.2 K in the 12 µm channel when compared to the ATSR-2 (Corlett, 2014; Smith, 2007). This offset is most likely a calibration issue that occurred post launch, and possible causes range from change in detector characteristics to changes in the SRF characteristics (position and shape).

The main objective of this paper is to estimate the trustworthiness of the AATSR and IASI-A for use in re-calibration by examining the full extent of the AATSR–IASI-A measurement biases over a wide range of scan angles, temperatures range (210 to 310 K), time (January 2008 to March 2011) and spectral (11–12 µm). Achieving this goal would help us in identification of scan-angles, time spans and geographic locations of observation that could be considered to be used as reference.

In the next section, we give a brief description of the ATSR-2, AATSR, AIRS and the IASI instruments along with the collocation algorithm that is used in this study to compare the two in-orbit references. This is followed by the results section. In the results section, we first address the issue of scan angle dependence of the AATSR and IASI-A biases. Following this, the temperature and time dependence of the AATSR and IASI-A biases are presented in addition to the impact of AATSR SRF shift on the temperature-dependent bias of the AATSR 12 µm channel. This section also evaluates the impact of changes in orbital parameters of ENVISAT on AATSR measurements and concludes by an independent analysis of spectral dependence of IASI-A bias. This study focuses on inter-comparison of 11 and 12 µm which are fully spanned by the IASI-A radiances. The IASI-A does not fully span the SRF of the 3.7 µm channel of the AATSR and the 3.6 µm of AVHRR and is therefore at this point not considered as a reference for its recalibration for this channel.

Inter-calibration a relative approach

While extensively used in monitoring contemporary instruments, inter-comparison between two in-orbit instruments such as that presented here has its limitations. A comparison between the AATSR and IASI-A does not provide enough evidence of their trustworthiness as a reference. By researching additional evidences this study would attempt to piece together evidences to zero in on goodness of the instruments and in case of anomalies, figure out the most likely source (AATSR or IASI-A) of the anomalies in the bias. In our analysis, this evidence is obtained (1) by comparing pre-launch characterization of the instruments with post launch inter-comparison results and by (2) independent inter-comparison with stable instruments, for example, with AIRS and ATSR-2. Several contemporary studies of IASI-A and AATSR such as Smith et al. (2012), Illingworth et al. (2009) etc are also cited extensively during the analysis.

2 Instrument description and collocation algorithm

2.1 Along-Track Scanning Radiometer (ATSR-2) and Advanced Along-Track Scanning Radiometer (AATSR)

The ATSR-2 (Along-Track Scanning Radiometer -2) and AATSR (Advanced Along-Track Scanning Radiometer) belong to the family of ATSRs (ATSR-1, ATSR-2 and AATSR) and were designed to aid climate studies (Llewellyn-Jones et al., 2001).

The ATSR-2 was launched in 1995 on board the ERS-2. It had three visible channels – 0.555, 0.659, and 0.865 µm, and three thermal channels – 3.7, 10.8, and 12 µm. It had an equatorial crossing time of 10:30 a.m. (within 30 min of AATSR). The Level 1B data sets for ATSR-2 are available from 1995 through 2003, which provides users the opportunity to intercompare the ATSR-2 with AIRS which started its operations in 2002.

The AATSR was an advanced version of the ATSR-2. It had four visible (0.555, 0.659, 0.865 and 1.61 µm) and three thermal bands (3.7, 11 and 12 µm). Its viewing principle and calibration mechanism is similar to ATSR-2. It was launched (onboard ENVISAT) in 2002 and operated until 8 April 2012.

In order to achieve their scientific goals of contributing to climate research these instruments aim to measure TOA to a very high level of accuracy. They use a highly sophisticated calibration mechanism (Llewellyn-Jones et al., 2001; Smith et al., 2001, 2012) to achieve this. This calibration mechanism uses two *Système international* (SI) traceable black bodies that are situated at either boundary of the sea surface temperature (SST range, approximately 253 and 305 K) as calibration references. Since these references are at either boundary they provide anchor points to estimate the effects of detector nonlinearity within the SST range. This reduces possible calibration errors maintaining high intrinsic sensitivity at the same time (Smith et al., 2001, 2012). The detectors themselves are maintained at a constant temperature of 80 K which ensures stability and keeps the radiometric noise at 270 K to within 0.05 K.

The ATSR-2 and AATSR have a conical scan and views a location at two zenith angles, once looking through the atmosphere at 55° zenith angle in the forward direction and a second time 3 min later but with a 0° zenith angle in time when it scans the same location in the nadir as a consequence of the satellites forward motion. This mode of scan produces two swaths of 500 km each; with a spatial resolution of 1 km × 1 km at nadir and 1.5 km × 2.0 km at the forward view, respectively. For the purpose of inter- comparison, we have used the AATSR Level 1B gridded data sets. This data set is the observed TOA radiance that is geo-located and resampled to 1 km × 1 km resolution everywhere (every pixel of forward as well as nadir views is 1 km × 1 km).

The two IR channels (11 and 12 µm) of the AATSR overlap the IR spectrum of IASI-A. Since both AATSR and IASI-A are morning/evening satellites and have equatorial crossing times within 30 min of each other, they provide a large amount of collocated pixels that are observed within a few minutes of each other. Similarly the 11 and 12 µm channels of ATSR-2 overlap with IR spectral of AIRS.

2.2 Infrared Atmospheric Sounding Interferometer (IASI-A)

The IASI-A is a hyper spectral instrument on board the MetOp-A . Launched in 2006, it measures the outgoing Earth radiance in IR bands (Phulpin et al., 2007; Clerbaux et al., 2007). It is recognized by GSICS as a benchmark for inter-satellite comparison of TOA radiance (e.g. Wu et al., 2009). It works on the principle of a Michelson's interferometer. It consists of a Fourier Transform Spectrometer with an imaging system which provides infrared spectra between 645 and 2760 cm^{-1} (3.6 to 15.5 µm) at a resolution of 0.25 µm (EUMETSAT, 2012). The IASI-A takes these observations in a step and stare mode and covers the ±47.85° FOV range in 30 steps during every 8.0 s scan cycle, with 3.3° for each step (normal mode). This means that the scan angle varies from [−47.85 to +47.85°].

IASI-A has a pixel resolution of 12 km at nadir with four pixels per view each positioned in the cross- and along-track directions located at ±0.825° from the centre point. The measured interferograms are processed by an onboard digital processing subsystem to reduce the data transmission rate. This subsystem also performs the radiometric calibration (based on the measurements of cold and warm reference targets, i.e. deep space and an onboard black body), and nonlinearity corrections. Once these data are received at the ground station, then the ground system processing takes over. The main components of the ground processing are radiometric post calibration, spectral calibration and apodization. The main output of this ground processing is a resampled, apodized, and calibrated spectrum with 8461 spectral samples. This product is known as the IASI-A level-1C radiance product, and is used as input to the collocation method described in the next subsection.

2.3 Atmospheric Infrared Radiometer Sounder (AIRS)

AIRS stands for Atmospheric Infrared Radiometer Sounder. It was launched on 4 May 2002 onboard the NASA's Aqua Satellite. It is a hyper spectral spectrometer with 2378 bands in the thermal infrared (3.7–15.4 µm) and 4 bands in the visible (0.4–1.0 µm). These ranges have been specifically selected to allow determination of atmospheric temperature with an accuracy of 1° K in layers 1 km thick, and humidity with an accuracy of 20 % in layers 2 km thick in the troposphere. The spectral ranges overlap with the AATSR and its predecessor the ATSR-2's (Along-Track Scanning Radiometer) 11 and 12 µm channels.

AIRS scans in the cross-track direction with a ±49.5° swath centred on the nadir which is followed by a rapid scan in 2/3 s taking routine calibration related data that consist of four independent cold space views, one view of the onboard black body calibrator, one view of the onboard spectral reference source, and one view of a photometric calibrator for the VIS/NIR photometer. Each scan line contains 90 IR footprints, with a resolution of 13.5 km at nadir and 41 km × 21.4 km at the scan extremes from nominal 705.3 km orbit. The Vis/NIR spatial resolution is approximately 2.3 km at nadir.

Table 1. Thresholds applied on collocated AATSR pixels in a single IASI pixel.

Thresholds	
Standard deviation of collocated pixels	< 0.5 K
Standard deviation of perimeter pixels	< 1 K
Time difference	< 15 min
Time span	January 2008–March 2011
Percentage of area of IASI pixel collocated with AATSR pixels	70 %
Sat zenith angle difference	1°

For the purpose of our study AIRS would be used as a transfer between the AATSR and ATSR-2 as its period of operation, and IR spectrum overlaps with both.

2.4 Collocation method

The purpose of a collocation algorithm is to identify pixel pairs (one from each sensor) where a given target is viewed by two sensors at nearly the same time under similar viewing conditions thus enabling a direct comparison of corresponding measurements. The accuracy and selection criteria of pixel pairs that are finally considered for comparison are fundamental parameters of a collocation algorithm. The latter has been discussed by Wu et al. (2009), wherein GSICS provided a baseline criterion for pixel pair selection during inter-comparison. Within the error bounds of geolocation errors, application of this criterion results in selection of scenes that are uniform, viewed with similar viewing angles around the same time. Thresholds for viewing angle and observation time differences are stated in Table 1. Selection of uniform scenes ensures that the effects of geolocation errors and effects of differing spatial resolution of the pixel pairs are minimized when their radiances are compared.

For the AATSR and IASI-A inter-comparison, a new collocation algorithm was developed that inherited some of the selection criteria from the GSICS baseline (Wu et al., 2009). This algorithm took the IASI-A (Level-1C) radiance data and AATSR (gridded Level-1B) orbital files as input and identified AATSR pixels of nadir and forward view that were collocated within the IASI-A pixel. In order to achieve a high degree of accuracy, the exact shape and size of the IASI-A pixel as it varied with scan angle was computed using standard trigonometric functions and used for the collocation.

This algorithm was used to identify AATSR:IASI-A collocated pixels from January 2008 through March 2011. For a given IASI-A:AATSR collocation, the IASI-A footprint on the ground is larger (12 km at nadir) than the AATSR (which is re-sampled to make it 1 km everywhere on the swath) so several AATSR pixels fall within each IASI-A pixel. In order to ensure scene uniformity within the IASI-A footprint, thresholds are set regarding the standard deviation (SD) of the AATSR pixels within the IASI footprint (Table 1). However setting this threshold alone does not guarantee that the state of the scene viewed by the two instruments remains homogenous and invariant when viewed by the two satellites. It is possible that clouds move into the IASI-A pixel within the threshold time (time between two satellite viewings of the same target) and break the homogeneity after the test is applied.

To ensure that such IASI-A pixels are identified and subsequently rejected, a second SD threshold test is applied. For this a perimeter area of five AATSR pixels around an IASI-A pixel (Fig. 1) is selected and the SD is computed for this set of AATSR pixels. Only those pixels for which the SD of perimeter pixels is also less than 1 K were selected for further comparison.

In the end the IASI-A spectrum for these collocations is integrated (convoluted) over the AATSR SRF (Eq. 1) to get IASI representative radiances. In this integration all the IASI-A radiances (denoted by IASI_RAD in Eq. 1) that fall within the range of (9.82–12.18) µm were used to get 11 µm IASI representative radiances and all the IASI-A radiances in the range (11.02–13.40) µm to get the 12 µm IASI representative radiances (IASI rep radiances). These wavelength ranges have been taken from the AATSR stated SRF ranges of the 11 and 12 µm channels. The radiances are then compared with the mean radiances of the AATSR that are collocated with the IASI-A pixel. Here IASI_RAD are the IASI-A radiances that fall within the wavelength band pass of AATSR.

Representative IASI-A radiances that have been computed by convoluting with the SRF of a target instrument with the aim of comparing for monitoring target instruments (as indicated in Eq. 1) have been widely used in GSICS community. Hewison et al. (2013) have argued that uncertainty due to spectral convolution is of the order of 0.01 K. This is smaller than calibration accuracy and would have little effect on the outcome of in-orbit inter-comparisons such as used here.

$$\text{IASI-A representative radiance} = \frac{\sum \text{IASI\_RAD} \cdot \text{SRF}}{\sum \text{SRF}} \quad (1)$$

This study also uses inter-comparisons of AIRS and ATSR-2 to investigate spectral dependence of IASI-A measurements (Sect. 3.5). These AIRS vs. ATSR-2 inter-comparisons are also made using a similar collocation method. In this case the AIRS radiances are convoluted over the ATSR-2 SRF to get ATSR-2 representative radiances. The thresholds in Table 1 are also same as used for AATSR vs. IASI-A.

However, it must also be pointed out that the AIRS (13:30 h equatorial crossing time) and ATSR-2 (09:30 equatorial crossing time) equatorial crossing times differ by more than several hours . The collocation algorithm was run for the AIRS and ATSR-2 for 3 months (from 1 September 2002 to 30 November 2002). It identified 767, 354 collocated pixels and 23, 305 pixels passed the threshold test (stated in

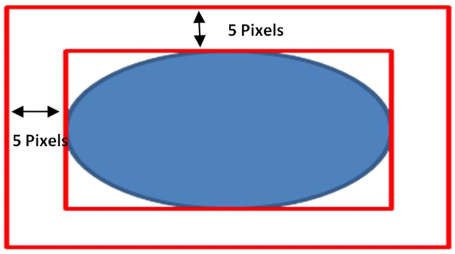

Figure 1. IASI-A foot print (blue) at nadir. The outer red boundaries indicate the perimeter area where the perimeter threshold is applied. This area is 5 AATSR pixels (5 km) wide. The mean radiance of AATSR pixels collocated within the blue is compared with the IASI-A representative pixel radiance.

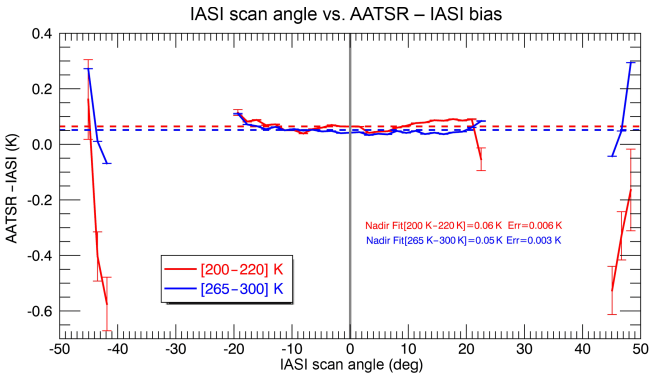

Figure 2. Scan angle dependence of the AATSR–IASI bias for cold (200–220 K) and SST (265–300 K) temperature ranges. Neither AATSR nor IASI show any scan angle dependence in the −20 to +20° scan angle range.

Table 1) and spanned the 240–280 K range enough for this inter-comparison to be useful as an independent reference for our study. Due to wide difference in equatorial crossing time, the collocations were mainly in located in higher latitudes. This has been summarized in Table 2.

Throughout this paper we have used IASI-A or AIRS representative radiances, i.e, IASI-A radiances convoluted with AATSR SRF for comparisons of AATSR with IASI-A and AIRS convoluted with ATSR-2 SRF for comparison of ATSR-2 with AIRS.

3 Collocation results

3.1 Scan angle dependence of AATSR–IASI-A bias

Measurement bias with respect to scan angle is a known phenomenon that has been displayed by instruments such as GOME (UV bands), AMSU (microwave bands) and AVHRR (IR bands, Snel, 2001; Tanzi, 2001; Wu, 2004; Wang and Cao, 2008; Mittaz and Harris, 2011). These instruments have been found to have scan angle dependencies in TOA measurements to varying degrees. The reasons for scan angle dependence are not always clear but in AVHRR it is hypothesized that it is due to the variation in polarization (Wang and Cao, 2008) that occurs when incident radiant flux originating from the target scene falls on the scan mirror at different angles while it is scanning (rotating). Since the root cause of this dependence is not fully understood, it is difficult to physically model it and as a result this dependence usually does not go away by employing a better calibration technique.

In its role as an in-orbit reference it is expected that inter-comparisons of IASI-A with concurrently flying instruments are able to reveal scan angle dependence of the measurements of the inter-compared instrument. In view of this the analysis of the scan angle dependence of AATSR–IASI-A aims to answer two questions (1) does the inter-comparison of IASI-A with AATSR show any evidence of scan angle dependence of IASI-A or the AATSR measurements? Earlier studies by Mittaz and Harris (2011) also detected scan angle dependence of AVHRR–IASI-A bias but It was not clear as to which instrument contributed most to this bias AVHRR or IASI-A . (2) Can the forward view of the AATSR act as a suitable in-orbit reference for IASI-A?

The 12 µm channel of AATSR has a known offset of 0.2 K. As will be shown later, it has complex temperature and time dependence so it is not used to measure the scan angle dependence.

Figure 2 shows the variation of AATSR–IASI-A 11 µm bias over the entire the scan angle range of IASI-A (i.e −47.85 to +47.85°) and AATSR scan angles in cold and SST temperature ranges.

While the bias in the scan angle range ±20° comes from the collocations between the nadir view of AATSR and the IASI-A, the biases beyond ±40° IASI-A scan angles come from collocations between the forward view of AATSR and the IASI-A. Both these views show different characteristics.

Figure 2 also shows that the AATSR–IASI-A bias at nadir view is nearly constant with some residual errors (~ 0.0025 K degree^{-1} of satellite zenith angle) and a constant offset of close to zero. Given the fact that the scan-angle-dependent variation of the bias at the nadir view is very small, the scan-angle-dependent bias between AVHRR and IASI-A seen by Mittaz and Harris (2011) is most likely an AVHRR effect and not an IASI-A effect.

As shown in Fig. 2, the bias between the AATSR forward view and the IASI-A seem to show a scan angle dependence in both temperature ranges (cold ~ 0.7 K and SST ~ 0.3 K). The following two important parameters need to be considered while analysing this bias. (1) The two instruments look at the same target pixel, but they look through different atmospheres. The AATSR forward views are measurements taken along track, while the IASI-A measurements are taken on targets across track. This can result in differing measurements of TOA radiance by the two instruments, and (2) the AATSR forward view has known geo-location errors. These errors are magnified at the poles.

Table 2. Number of collocations produced by the collocation algorithm for AATSR vs. IASI-A inter-comparison and ATSR-2 vs. AIRS inter-comparison (second last column). The last column displays the number of collocations obtained after applying threshold stated in Table 1 that are eventually used in this study.

Collocation	Period of collocation	Number of collocations	Number of qualifying collocations used in this study
AATSR vs. IASI-A	1 January 2008–31 March 2011	10, 047, 594	1, 447, 030
ATSR-2 vs. AIRS	1 September 2002–30 November 2002	767, 354	23, 305

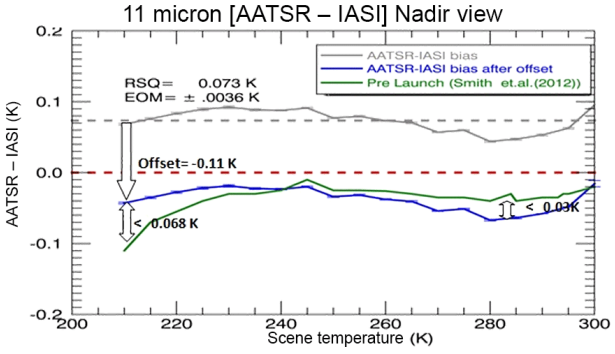

Figure 3. Temperature dependence of AATSR–IASI-A (in grey) bias over the period of 39 months. Blue curve is the same temperature dependence with an offset of 0.11 K (i.e. post launch) subtracted from it. This blue curve is similar to pre-launch (Smith et al., 2012) characteristics of AATSR to within hundredth of a kelvin.

Corlett (2014) noted alignment issues with the AATSR forward view, wherein the forward-view minus nadir-view image shows significant edge effects around eddy structures and also at the edges of clouds. Such alignment issues lead to geo-location errors in the forward view particularly at cloud edges which are characterized by low temperature (temperatures < 240 K). Hence forward view of the AATSR is not suitable to act as in orbit reference. In the analysis presented in this paper only nadir view of AATSR is considered in evaluating the AATSR–IASI-A biases.

3.2 Temperature dependence of the AATSR–IASI-A bias

3.2.1 11 µm

Figure 3 shows the variation of AATSR–IASI-A biases over a temperature range of 210–300 K computed from all the pixels irrespective of their location (land/ocean) and time of observation (day/night). The temperature range chosen here (210–300 K) is similar to the range used by Smith et al. (2012) to depict the difference between the temperature measured by the AATSR and that of a black body that it observed during pre-launch testing (green curve in Fig. 3). This temperature range also includes the range (275–300 K) used by Illingworth et al. (2009) to study the AATSR–IASI-A difference. Hence the choice of this range gives us the opportunity to compare and verify the inter-comparison results with two independent studies, one conducted at pre-launch and the other carried out post-launch with limited sample size.

The AATSR–IASI-A bias variation in the 210–300 K range is similar to the difference that was observed by Smith et al. (2012), during the pre-launch testing. The characteristic dip at the low temperature (< 230 K) and the hump at 245 K are captured well. If one applies an offset of −0.11 K to the AATSR–IASI-A variation curve, the pre-launch and the post launch (i.e. our inter-comparison) variations match to within a few hundredths of a degree kelvin.

Since the AATSR pre-launch calibration has a known negative bias of the order of 0.0–0.05 K referenced to SI calibrated sources, and the inter-comparison of AATSR–IASI-A shows a positive bias of the order of 0.07 K (Fig. 3), the observed positive AATSR–IASI-A bias (grey curve in Fig. 3) is likely to be an IASI-A bias relative to the AATSR. Since in the SST temperature regime the AATSR is thought to be absolutely accurate to a few hundredths of a degree, the implication is that IASI-A (when corrected for this small bias) can generate radiances that are almost as accurate as pre-launch data to within a few hundredths of a degree kelvin.

The −0.11 K offset has been computed by minimizing the root mean square (RMS) difference between the pre-launch and the post launch (AATSR–IASI-A) curve. A series of RMS difference between post and pre-launch values was calculated by adding successively 0.001 K offsets to IASI-A temperature and reducing the AATSR-IASI bias. The minimum value of RMS differences occurs at an offset of −0.11 K.

Our inter-comparison results are in agreement with the AATSR–IASI-A comparisons of Ilingworth et al. (2009) to a level of a few hundredths of degree. While our mean difference over the entire temperature range is 0.073 K (± 0.03 K), Illingworth et al. (2009) difference is of the order of 0.05 K (±0.03 K). The small difference between the two comparisons can be attributed to the difference in data sets.

3.2.2 12 µm

Immediately after the launch of the AATSR onboard ENVISAT it was found that the 12 µm channel had an apparent

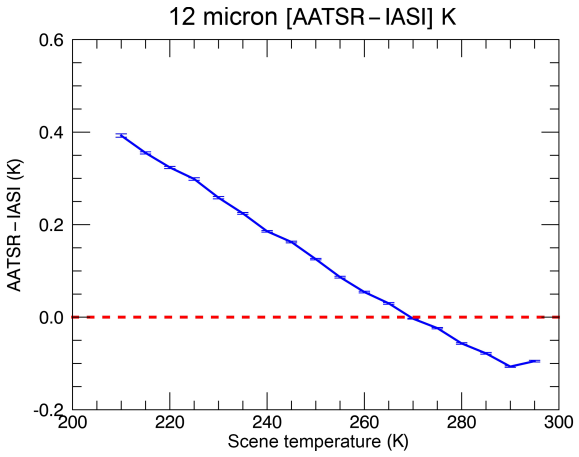

Figure 4. Temperature-dependent bias of the AATSR-IASI-A for the 12 µ channel.

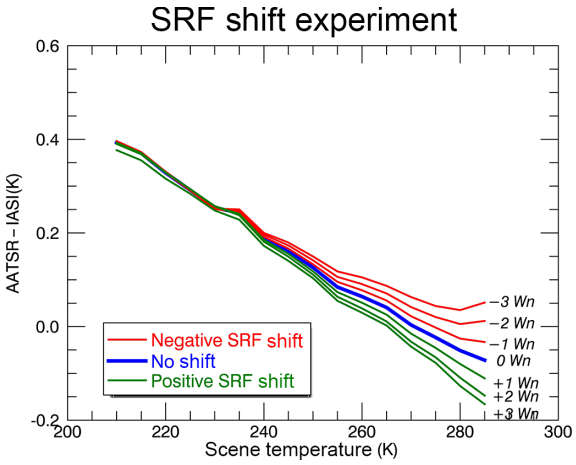

Figure 5. Impact of shifting the AATSR spectral response function by three wave numbers on either side of its central wave number (Wn) position in steps of 1 Wn. The scene-temperature-dependent nature of AATSR-IASI-A bias does not diminish by shifting SRF.

BT offset of ~ -0.2 K in the SST temperature range when compared with the ATSR-2 (Corlett, 2014). It was verified by Smith (2007) to be an AATSR artifact.

However, our analysis has found that the BT offset is strongly temperature-dependent and steadily grows to about 0.4 K as the temperatures decreases to 210 K (Fig. 4). In the SST temperature range the bias is negative. Taking into account the small (0.07 K) IASI-A bias discussed above, this is approximately consistent with the previously known bias of -0.2 K. Among the possible reasons of this effect is that the SRF may have undergone a shift or a possible long wave leak developed post launch (Smith, 2007).

We have investigated the possibility of estimating a simple SRF shift to explain the bias by undertaking a set of experiments. The SRFs were shifted by $\pm n$ wave numbers (where $n = 1, 2, 3$). Figure 5 shows the impact of shifting the SRF on the AATSR–IASI bias for each "n". As shown in Fig. 5, the temperature dependence of the bias is preserved right up until a shift of $+3$ wave numbers is applied. A similar conclusion was drawn with the -3 shifts, and the overall conclusion is that SRF shift is an unlikely solution to the temperature-dependent bias.

Further investigation into possible causes of the bias is beyond the scope of this study. The bias variation shown in Fig. 4 also shows that the error bars are small. The maximum value of the error bar is ± 0.0023 K which indicates that the bias is highly stable and can be empirically corrected by fitting a polynomial function.

3.3 Temporal dependence of AATSR–IASI-A biases

Legacy instruments such as the AVHRR are known to show seasonal variation in radiance measurements. This variation is mainly attributed to seasonal variation in instrument temperature. Mittaz and Harris (2011) have shown that this seasonal effect can be corrected by using a better calibration scheme that physically models the effects of seasonal changes in instrument temperature. However, this scheme needs stable references that are minimally impacted by instrument temperature. Since IASI-A and AATSR are envisaged to be used as references in the AVHRR re-calibration, it is vital to understand and quantify the seasonal variation in the measurement.

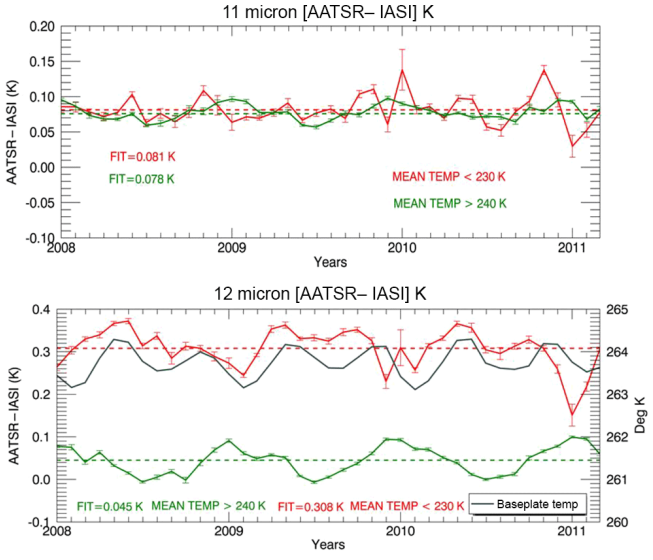

Figure 6. Time series of variation of AATSR–IASI bias for 11 and 12 µm channels in the cold (red) and warm (green) temperature ranges. The bias at cold temperature in 12 µm is correlated ($\rho = 0.78$) with the instrument baseplate temperature (grey curve in the lower plot).

Here we investigate temporal variation of the AATSR–IASI-A bias on warm (BT > 240K) and cold (BT < 230 K) temperature ranges. The warm range spans most of the tem-

perature range that lies between the warm and the cold black body. The cold temperature range (BT < 230 K) is chosen deliberately away from this temperature range as it is likely to have a reduced impact of the robust calibration scheme.

3.3.1 Warm temperature range (temp > 240 K)

The temperature of the two calibration black bodies in the AATSR instrument lie in the warm temperature range at 260 K cold and 310 K warm. This helps in pinning down the effect of detector nonlinearly and ward off effects of seasonal changes in instrument temperature. The robustness of this calibration system is clearly demonstrated when month-to-month AATSR–IASI-A bias was analysed. As seen in Fig. 6, the 11 µm channel maintains a very well-calibrated stance with small annual deviations (±0.01 K) around its mean value of 0.078 K.

The 12 µm channel of AATSR–IASI-A bias shows slightly larger amplitude (0.045 ± 0.032 K) than the 11 µm channel, in this temperature range. Despite the known temperature-dependent BT offset (Fig. 6) of this channel, the calibration mechanism ensures that the seasonal variability in the AATSR–IASI bias at the warm temperature range remains confined to less than a few hundredths of a degree K. So the seasonal variation in the bias for warmer temperatures ($T > 240$ K) in both of the channels can be estimated as very small (a few hundredths of degree).

3.3.2 Cold temperature range (temp < 230 K)

The cold temperature range lies outside of the temperature range spanned by the two calibration black bodies of the AATSR which are situated at roughly 250 and 305 K. The AATSR has a calibration bias (see green curve in Fig. 3, Smith et al., 2012) below 230 K that grows to −0.1 K. A similar characteristic dip is displayed post launch when AATSR is compared with IASI-A over several months (Fig. 3). This inter-comparison shows that the 11 µm channel (Fig. 6) bias for colder BTs is slightly higher than that seen for the warmer BTs, and hovers around 0.081 K (±0.022 K).

A similar analysis of the 12 µm channel AATSR–IASI bias reveals a larger seasonal variation of 0.31 K (±0.03 K) as compared to the 11 µm. Within a given year there are two distinct peaks. For this channel, the entire AATSR–IASI bias curve is closely cross correlated (Fig. 6) with the instrument base plate temperature variation (cross correlation = 0.78) thereby indicating that the instrument temperature could be influencing the AATSR measurements in the colder temperature range for this channel.

In the 11 µm channel, some months (November and December) show spikes of the order of 0.15 K that stand out. Since these spikes occur during the time of "year end orbit maneuver of ENVISAT" (Noll, 2010) it is likely that these are caused by temporary AATSR geo-location errors and not calibration errors of the AATSR or the IASI-A.

For 2008 and 2009 these spikes are nearly the same however the spike in end of 2010 appears unique as it is followed by an anomalous dip in January 2011.

Impact of ENVISAT orbit lowering maneuver in 2010

It must also be noted that the orbit maneuver carried out in October 2010 was different from the ones carried out in prior years because orbital inclination control was switched off and the altitude of the satellite was reduced by 17.4 km (Miranda et al., 2010). This led to a new 30-day repeat cycle (431 orbits per cycle), instead of the earlier 35-day repeat cycle (501 orbits per cycle). It was expected that this would not cause any anomalies in AATSR measurements and initial testing immediately after the maneuver did not detect any anomaly (Cocevar et al., 2011).

However it must be noted that changes in orbital inclination are slow and their impacts would not be visible in the first few orbits that were used in the testing phase (Cocevar, 2013) and might be detectable only in the subsequent months. By extending the inter-comparison several months beyond October 2010 (i.e. until March 2011) our inter-comparison study was able to detect the impact of this maneuver (Fig. 6) on AATSR measurements as a spike that starts in November 2010 and lasts till February 2011.

Since such spikes can impact the AVHRR recalibrating process, we investigated the full scale of these spikes. Figure 7 shows the temperature dependence of AATSR–IASI-A bias for the DJF for the 11 and 12 µm channels. This figure shows that while the 2008 and 2009 spikes show small deviations at the cold temperature end the bias for 2010–2011 shows a clear temperature-dependent trend.

These deviations in 2011 are important as they can impact the re-calibration of the AVHRR from 2011 onwards if AATSR is to be used as a reference for this period. Further analysis (Fig. 8) showed that these deviations are largest for collocations between the AATSR and IASI-A over Greenland. Figure 8 also shows the biases for the same months (DJF) when Greenland data are excluded and one can see that the deviations are reduced.

Given that AATSR's onboard calibration has worked well prior to this maneuver and has even replicated pre-launch behaviour for months prior to October 2010, the deviations seen here do not appear to be a calibration issue as change in orbital parameters would not be able to influence the robust onboard calibration scheme. This trend could be due to small number of collocations over this area or could also be due to geolocation errors that manifest themselves when the inclination control is switched off and satellite orbit is lowered thereby changing the observation geometry. More investigation is required to reveal the cause of this anomaly.

It must be noted that a similar trend is not found in the diametrically opposite position in the Southern Hemisphere where the SNO (simultaneous nadir overpass) between AATSR and IASI-A also overlap under similar con-

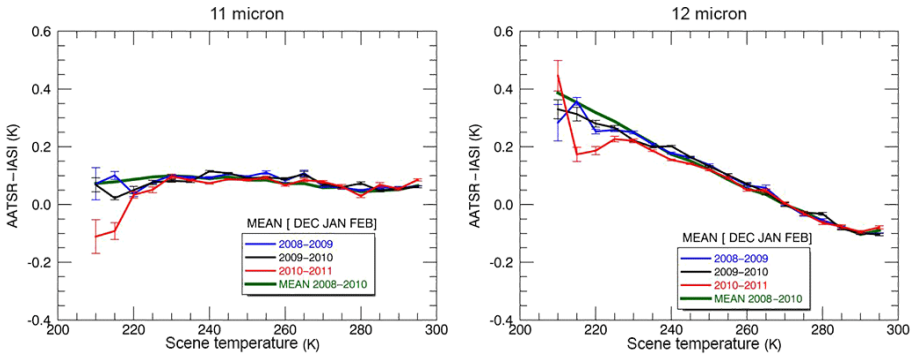

Figure 7. Year to year AATSR–IASI bias for DJF for the 11 and 12 µm channels. An anomalous trend at cold temperature is clearly visible in November 2010 DJF.

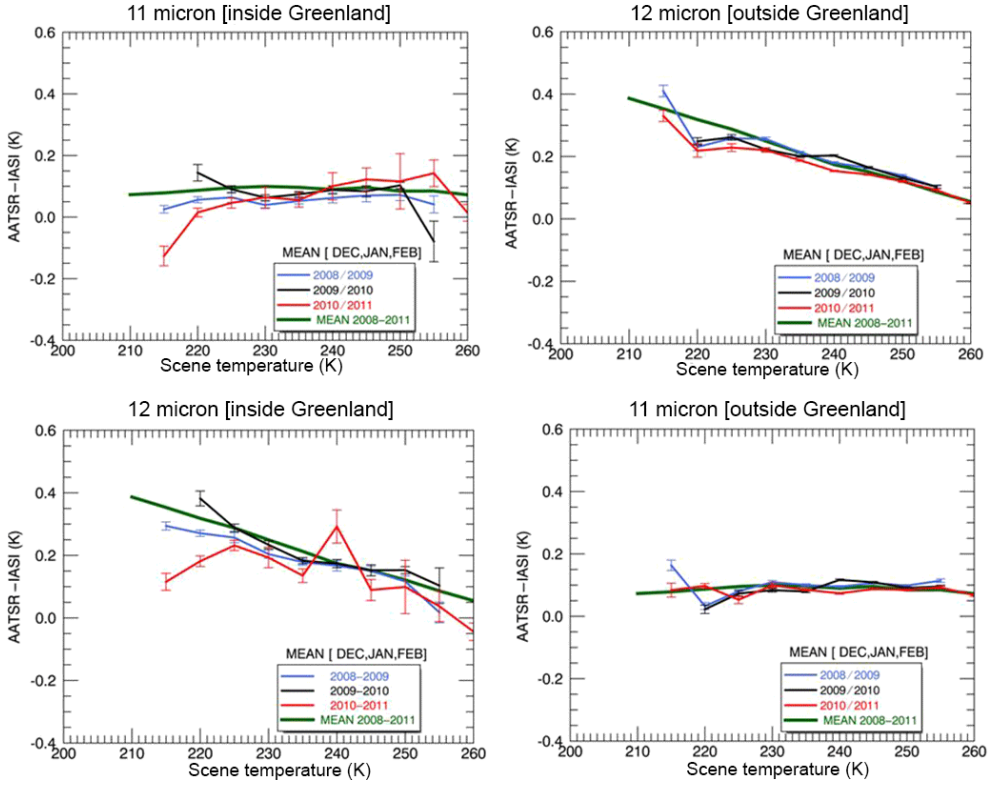

Figure 8. Comparison of AASR–IASI-A bias over Greenland and outside Greenland. The anomalous trend seen in November 2010 DFJ AATSR–IASI bias is mainly confined to Greenland.

ditions as they do over Greenland. All the collocations between 60 and 82° S occur over ocean. Since spatial temperature gradients over the oceans are not as sharp as those over land (i.e. neighbouring pixels have nearly the same temperature value), any offsets in those pixel location due to errors in geo-location would not show up as a temperature bias.

3.4 Spectral dependence of AIRS and IASI-A measurements.

Due to the anomaly in the AATSR 12 µm channel the AATSR–IASI-A inter-comparison does not give a credible evidence of spectral dependence of IASI-A measurements. From a re-calibration standpoint it would be vital to know if such dependence exist and quantify them should there be any. Such dependence if not properly corrected can leave signatures in the AVHRR re-calibrated series.

Table 3. Summary of AATSR vs. IASI-A inter-comparison. The table shows the measurements of the two instruments agree with each other.

Channel	Scan angle	Temperature	Temporal	Spectral
11 Micron	No scan angle dependence AATSR, forward view not recommended to be used as a reference.	AATSR and IASI-A agree to within 0.07 K and bias variation similar to pre-launch AATSR behaviour.	No evidence of temporal trends in a 39-month period of study.	It is likely that IASI-A has a small spectral dependence bias of ~ 0.02 K. Routine monitoring of this bias is recommended.
12 Micron	n/a	Varies from [0.4 to −0.2 K] over scene temperature range [220–300 K]	No evidence of temporal trends in a 39-month period of study.	

n/a: not applicable.

Earlier studies by Wang et al. (2010, 2011) compared IASI-A with AIRS (IASI-A–AIRS) using direct SNO as well as by using GOES-11 as a transfer. These studies conclude that the AIRS vs. IASI-A bias has small temperature as well as spectral dependence. Wang et al. (2011) indicate that the bias is of the order of −0.042 K (±0.05 K) and −0.093 K (±0.05 K) for 11 and 12 µm for cold (i.e less than 240 K) temperature. For warm (more than 260 K) temperature bias is −0.029 K (± 0.01 K) and −0.043 K (±0.01 K) for 11 and 12 µm channels. All uncertainties are at 95 % confidence level. Though the study suggested a difference in the AIRS–IASI-A bias from 11 to 12 µm which indicated a small spectral bias between the two, the study also suggested further analysis to concretize this bias in order to use it for climate purposes. It was also not clear weather AIRS or IASI-A or both caused the spectral dependence bias seen in this study.

Using collocation data produced from 3 months of SNO inter-comparison of AIRS and ATSR-2, we examined the AIRS biases with ATSR-2. It was found that they agree to within −0.015 K (±0.001 K) in 11 µm and −0.011 (±0.004 K) 12 µm channels. The ATSR-2 is a satellite belonging to the AATSR family and has no known inter-channel-dependent bias and as stated earlier measures TOA to a high level of accuracy. Hence it is likely that IASI-A is contributing more (than AIRS) to the AIRS vs. IASI-A bias found in the Wang et al. (2012) study and needs to be accounted for when using IASI-A as a reference.

3.5 Other dependencies of AATSR–IASI-A bias

Mittaz and Harris (2011) have shown that in instruments such as the AVHRR have significant diurnal biases that result from heating and cooling of the instrument as the satellite moves from sunlit to non-sunlit sides over an orbit. For instruments (such as AATSR and IASI-A) that are candidates for being used as in-orbit references it is important that such diurnal variations are quantified. The dependence of AATSR–IASI-A vs. scene temperature biases on scene selection (land/sea and day/night scenes) over the entire 39-month period of collocation was also investigated. It was found that a significant number of collocation pixels were rejected when additional scene selection criterion was applied together with those thresholds stated in Table 1. This only influenced random noise associated with the AATSR–IASI-A bias and does not impact our conclusions of the AATSR–IASI-A bias variation with respect to scene temperature and it remains similar to pre-launch behaviour. This demonstrated the robustness of the onboard calibration of the two instruments and their ability to resolve diurnal variations in measurements when used as references and compared with other instruments.

However, specific events such as orbital maneuvers have had some impact AATSR–IASI-A bias on specific scene locations (such as Greenland) and these spots would be eventually ignored while constructing the reference radiance.

4 Conclusions

Using AATSR and IASI-A collocations spanning 39 months (January 2008–March 2011) this study measures the trustworthiness of AATSR and the IASI-A. The idea is to eventually use these instruments as in-orbit reference for recalibration of the AVHRR series of instruments (Mittaz and Harris, 2011). This study focuses on the 11 and 12 µm channels only.

This trustworthiness is measured by evaluating several parameters. These are the following: (1) similarity between pre-launch temperature-dependent bias (Smith et al., 2012) of AATSR and post launch temperature dependence of AATSR–IASI-A bias as shown in Fig. 2, (2) scan angle dependence of AATSR–IASI-A bias, (3) scene temperature dependence of bias, and (4) time dependence of the AATSR–IASI-A bias, (5) spectral dependence of bias AATSR–IASI bias. Results of our analysis are summarized in Table 3.

Our study indicates (Table 3) that both AATSR and IASI-A are stable instruments that show no evidence of scan angle dependence of measurements, no temporal trends during the

period of study and a very small spectral dependence of measurement bias in the IASI-A. In fact, for the 11 µm channel, the AATSR retains its characteristic pre-launch behaviour (Fig. 3) and the IASI-A is nearly as good as a pre-launch reference (plus an offset of 0.07 K). Also the 12 µm AATSR bias is temperature-dependent but stable and can be empirically corrected. Hence these instruments can act as trustworthy reference however care needs to be taken while generating long term reference records for recalibration purposes. In addition the study answers three more questions that are vital to their use as a reference for AVHRR re-calibration.

Our study answers a long pending question posed by studies such as by Blumstein et al. (2007), Wang and Cao (2008) and later by Mittaz and Harris (2011) which detected scan angle bias in AVHRR and IASI-A inter-comparison and it was not conclusively known by these studies which of the two instruments contributed to the scan angle bias. The AVHRR has scan-angle-dependent bias at cold temperature range (210–240 K).

Our study provides evidence that IASI-A has a small spectral dependence with respect to AIRS. This varies by a few hundredth of a kelvin from 11 to 12 µm. Given that later IASI's like IASI-B have detected spectral bias (Jouglet, 2016). In order to use it as a reference it is vital to monitor this bias and apply corrections when needed.

Our study reveals that ATSR-2-AIRS bias is -0.015 K (± 0.001 K) in 11 µm and -0.011 (± 0.004 K) 12 µm channels. These biases are small and no evidence of temperature, time and spectral dependence in this bias was found; hence AIRS can act as an perspective to bridge ATSR-2 with AATSR, which can help provide a long time series of reference radiance for the AVHRR recalibration.

Recommendations for using AATSR and IASI-A as a reference.

In order to use AATSR and IASI-A as reference we need to know the conditions under which the AATSR and IASI-A give the most credible radiances. Based on the analysis presented in this study we have the following recommendations for generating reference radiances.

1. It is recommended that only nadir view of AATSR is used as reference and forward view is not used as a reference.

2. It is recommended that post the orbital maneuver of ENVISAT in October 2010 only mid and lower latitudes TOA measured by AATSR should be used. AATSR TOA data over Greenland should be excluded from being used as a reference.

3. The AATSR and IASI-A match to hundredth of a kelvin in the SST temperature range. Outside this range their agreement drops to a tenth of a kelvin. Empirical corrections should be applied to the AATSR 11 and 12 µm. A sixth degree polynomial is a good fit to temperature dependence of the 12 µm bias. Further, independent estimates of AATSR and IASI-A should also be made (such as IASI-A comparison with AIRS and ATSR-2 comparison with AIRS).

4. Since 12 µm AATSR also has a cold bias that seasonally varies (Fig. 6), the cold temperature range for this channel should either be ignored or be used with caution while re-calibrating AVHRR.

5. Information from routine instrument monitoring reports (such as ENVISAT Cycle reports) and IASI-A Quarterly Performance Reports in "Observation" presented on CNES website: https://iasi.cnes.fr/en/IASI/lien1_car_instr.htm, need to be routinely analysed to identify the cause of measurement anomalies and identify times and location of best instrument behaviour. These reports can help select time and geographic locations and help reveal vital parameters of the reference instrument such as spectral bias (Jouglet, 2016) or deviations in the onboard calibration mechanism etc.

Acknowledgements. We wish to thank Bob Kuligowski, Lawrence E. Flynn, Sriharsha Madhavan at NOAA/STAR, and Richa Mathur for proofreading and help improving this article. Thanks are also due to Andy Harris at NOAA/STAR for providing the IASI-A footprint shapes and also for providing vital information on the ATSR-2 and AATSR calibration. Thanks are also due to Fuzhong Weng for supporting the publication of this paper.

Edited by: A. Richter
Reviewed by: three anonymous referees

References

Blumstein, D., Tournier, B., Cayla, F. R., Phulpin, T., Fjortoft, R., Bull, C., and Ponce, G.: Inflight performance of the Infrared Atmospheric Sounding Interferometer (IASI) on Metop-A, P. SPIE, 6684, 66840H, doi:10.1117/12.560907, 2007.

Cocevar, P.: ENVISAT – AATSR CYCLIC REPORT #98, ESA, 1–19, available at: https://earth.esa.int/sppa-reports/envisat/aatsr/cyclic/2010-12-26/AATSR_CR_98_101226_110125.pdf (last access: 14 September 2015), 2011.

Cocevar, P.: IDEAS – Envisat AATSR Performance Report, IDEAS-VEG-OQC-REP-1143, ESA, 1–46, available at: https://earth.esa.int/documents/10174/437508/Envisat_AATSR_Performance_Report.pdf (last access: 14 September 2015), 2013.

Corlett, G. K.: (A)ATSR Validation Activities, available at: http://atsrsensors.org/pdf/ATSRValidationIssues.pdf (last access: 14 September 2015), University of Leicester, UL- AATSR-VIR, 5B, 2014.

Clerbaux, C., Hadji-Lazaro, J., Turquety, S., George, M., Coheur, P. F., Hurtmans, D., Wespes, C., Herbin, H., Blumstein, D.,

Tournier, B., and Phulpin, T.: The IASI/MetOp Mission: first observations and highlights of its potential contribution to GMES, Space Research Today, 168, 19–24, 2007.

EUMETSAT: IASI Level 1 Product Guide, Ref: EUM/OPS-EPS/MAN/04/0032, Issue v3j, EU- METSAT, 1–110, available at: http://www.eumetsat.int/website/wcm/idc/idcplg?IdcService=GET_FILE&dDocName=pdf_iasi_level_1_prod_guide&RevisionSelectionMethod=LatestReleased&Rendition=Web (last access: 14 September 2015), 2012.

Hewison, T. J., Wu, X., Yu, F., Tahara, Y., and Koenig, M.: GSICS inter-calibration of infrared channels of geostationary imagers using Metop/IASI, IEEE Trans. Geosci. Remote Sens., 51, 3, 1056–1080, 2013.

Illingworth, S. M., Remedios, J. J., and Parker, R. J.: Intercomparison of integrated IASI and AATSR calibrated radiances at 11 and 12 µ, Atmos. Chem. Phys., 9, 6677–6683, doi:10.5194/acp-9-6677-2009, 2009.

Jouglet, D.: IR hyperspectral comparisons, GSICS Annual Meeting 2016, Tokyo, Japan, available at: http://gsicswiki.net/pub/Development/20160229/3p_Jouglet_IR_hyperspectral_comparisons.ppt, last access: 14 May 2016.

Llewellyn-Jones, D., Edwards, M. C., Mutlow, C. T., Birks, A. R., Barton, I. J., and Tait, H.: AATSR: global-change and surface-temperature measurements from Envisat, ESA Bull.-Eur. Space, 105, 11–21, 2001.

Miranda, N. Duesmann, B., Pinol, M., Giudici, D., and D'Aria, D.: Impact of the Envisat Mission Extension on SAR data, available at: http://earth.esa.int/pub/ESA_DOC/ENVISAT/Impact_of_Envisat_Mission_Extension_on_SAR_data_-_1_01.pdf (last access: 12 September 2015), 2010.

Mittaz, J. P. D. and Harris, A. R.: A physical method for the calibration of the AVHRR/3 thermal IR channels. Part II: An in-orbit comparison of the AVHRR long wave thermal IR channels on board MetOp-A with IASI, J. Atmos. Ocean. Tech., 28, 1072–1087, 2011.

Noll, C. E.: The Crustal Dynamics Data Information System, a resource to support scientific analysis using space geodesy, in: DORIS Special Issue: Scientific Applications in Geodesy and Geodynamics, edited by: Willis, P., Adv. Space Res., 45, 1421–1440, doi:10.1016/j.asr.2010.01.018, 2010.

Ohring, G., Wielicki, B., Spencer, R., Emery, B., and Datla, R.: Satellite instrument calibration for measuring global climate change – report of a Workshop, B. Am. Meteorol. Soc., 86, 1303–1313, 2005.

Phulpin, T., Prel, F., Blumstein, D., Tournier, B., Prunet, P., and Schlüssel, P.: Applications of IASI on MetOp-A: first results and illustration of potential use for meteorology, climate monitoring, and atmospheric chemistry, Proc. SPIE, 6684, 66840F, doi:10.1117/12.736816, 2007.

Smith, D. L.: Effect of long wavelength response in AATSR filters on brightness temperature measurements, AATSR Technical Note, PO-TN-RAL-AT-0541, Issue 1.0, Rutherford Apple- ton Laboratory, 2007.

Smith, D. L., Delderfield, J., Drummond, D., Edwards, T., Mutlow, C., Read, P., and Toplis, G.: Calibration of the AATSR instrument, Adv. Space Res., 28, 31–39, 2001.

Smith, D., Mutlow, C., Delderfield, J., Watkins, B., and Mason, G.: ATSR infrared radiometric calibration and in-orbit performance, Remote Sens. Environ., 116, 4–16, 2012.

Snel, R.: In-orbit optical path degradation: gome experience and sciamachy prediction, in: Proceedings of the ERS-ENVISAT Symposium, ESA Publications Division, Nordwijk, the Netherlands, SP-461 (on CD ROM), 16–20 October 2000, Gothenburg, Sweden, 2001.

Tanzi, C. P.: Degradation of UV earth albedo observations by Global Ozone Monitoring Experiment (GOME), in: Proceedings of the ERS-ENVISAT Symposium, ESA Publications Division, Nordwijk, the Netherlands, SP-461 (on CD ROM), 16–20 October 2000, Gothenburg, Sweden, 2001.

Wang, L. and Cao, C.: On-orbit calibration assessment of AVHRR longwave channels on MetOp-A using IASI, IEEE T. Geosci. Remote, 46, 4005–4013, doi:10.1109/TGRS.2008.2001062, 2008.

Wang, L., Wu, X., Goldberg, M., Cao, C., Li, Y., and Sohn, S.-H.: Comparison of AIRS and IASI radiances using GOES imagers as transfer radiometers toward climate data records, J. Appl. Mete. Climatol., 49, 478–492, doi:10.1175/2009JAMC2218.1, 2010.

Wang, L., Goldberg, M., Wu, X., Cao, C., Iacovazzi Jr., R. A., Yu, F., and Li, Y.: Consistency assessment of Atmospheric Infrared Sounder and Infrared Atmospheric Sounding Interfer ometer radiances: double differences versus simultaneous nadir overpasses, J. Geophys. Res., 116, D11111, doi:10.1029/2010JD014988, 2011.

Wu, D. L.: Mesoscale gravity wave variances from AMSU-A radiances, Geophys. Res. Lett., 31, L12114, doi:10.1029/2004GL019562, 2004.

Wu, X., Hewison, T., and Tahara, Y.: GSICS GEO-LEO intercalibration: Baseline algorithm and early results, Proc. SPIE, 7456, 745604-1–745604-12, 2009.